

2D and 3D Supramolecular Structures via Hydrogen Bonds and π -Stacking Interactions in Arylsulfonates of Nickel and Cobalt

Felipe Gándara, Carlos Fortes-Revilla, Natalia Snejko, Enrique Gutiérrez-Puebla, Marta Iglesias, and M. Angeles Monge*

Instituto de Ciencia de Materiales de Madrid, CSIC, Sor Juana Ines de la Cruz 3, Cantoblanco, 28049 Madrid, Spain

Received May 23, 2006

Five novel arylsulfonates of Ni and Co have been hydrothermally obtained and their structures determined by X-ray single-crystal diffraction. $[\text{Ni}(\text{Phen})(\text{H}_2\text{O})_4](1,5\text{-NDS})\cdot 2\text{H}_2\text{O}$ (**1**) is a hydrogen-bonded supramolecular layered compound formed by self-assembly of tetraaqua-*o*-phenanthrolinenickel(II) cations and 1,5-naphthalenedisulfonate anions, $[\text{Ni}(\text{Phen})_2(\text{H}_2\text{O})(1,5\text{-NDS})]$ (**2**) and $[\text{Ni}(\text{Phen})_2(\text{H}_2\text{O})(2,6\text{-NDS})]\cdot 2\text{H}_2\text{O}$ (**4**) exhibit 2D structures via O–H \cdots O and π – π (both perfect face-to-face and parallel-displaced) stacking interactions, $[\text{Co}(\text{Phen})_2(\text{H}_2\text{O})(1,5\text{-NDS})]\cdot 2\text{H}_2\text{O}$ (**5**) presents a 3D structure via O–H \cdots O hydrogen-bond layers and π – π parallel-displaced stacking interactions, and $[\text{Co}(\text{Phen})_2(1,5\text{-NDS})]$ (**3**) is the first example of a covalently bonded polymeric cobalt sulfonate. Its 1D structure comprises chains formed through bitopic 1,5-NDS linkers. Rates and selectivities for oxidation of organic sulfides with H_2O_2 were measured with **2**–**5**.

Introduction

The sulfonate group RSO_3^- bears a strong structural analogy to the phosphonate group RPO_3^{2-} . Metal phosphonates represent a broadly studied class of solids.¹ In contrast, because of the perception that the sulfonate is a poor ligand, sulfonates as spacers for functional extended networks have only been examined to a considerably small extent.^{2,3} There are some examples of works on the supramolecular chemistry of the sulfonate group in extended solids built up by cooperative coordination and other weak intermolecular interactions,⁴ and this has been recently reviewed.⁵ There are also some examples in the literature with the RSO_3^- group, where R is 1,5-NDS and 2,6-NDS (NDS = naphtha-

lenedisulfonate). Structures of compounds of group 1 and 2 metal ions with 1,5-NDS, namely, $[\text{M}_2(1,5\text{-NDS})(\text{H}_2\text{O})_2]$ ($\text{M} = \text{Li}^+, \text{Na}^+, \text{and } \text{K}^+$) and $[\text{M}(1,5\text{-NDS})(\text{H}_2\text{O})_n]$ ($\text{M} = \text{Mg}^{2+}, \text{Ca}^{2+}, \text{Sr}^{2+}, \text{and } \text{Ba}^{2+}$), are found.⁶ Most of the transition-metal sulfonates obtained from an aqueous solution are aqua-metal sulfonate salts,⁷ by the introduction of other ligands as auxiliaries to the metal centers, sulfonate anions can compete with water molecules and coordinate to transition metals.⁸ For example, coordination polymers of Cd^{2+} and Cu^{2+} with 1,5- and 2,6-NDS are formed with the addition of amino ligands.^{9,10} It is worth pointing out that, in the case of Ni^{2+} and Co^{2+} , most of the sulfonate compounds obtained

* To whom correspondence should be addressed. E-mail: amonge@icmm.csic.es. Tel: +34-91-334-9000. Fax: +34-91-372 06 23.

- (1) Clearfield, A. *Prog. Inorg. Chem.* **1998**, *47*, 371. Dom, T.; Chamayou, A. C.; Janiak, C. *New J. Chem.* **2006**, *30*, 156.
- (2) Gunderman, B. J.; Squattrito, P. J. *Inorg. Chem.* **1995**, *34*, 2399.
- (3) Gunderman, B. J.; Squattrito, P. J. *Inorg. Chem.* **1994**, *33*, 2924. Haynes, J. S.; Sams, J. R.; Thompson, R. C. *Can. J. Chem.* **1981**, *59*, 669. Arduini, A. L.; Garnett, M.; Thompson, R. C.; Wong, T. C. T. *Can. J. Chem.* **1975**, *53*, 3812. Cai, J.; Chen, C. H.; Liao, C. Z.; Yao, J. H.; Hu, X. P.; Chen, X. M. *J. Chem. Soc., Dalton Trans.* **2001**, 1137.
- (4) Shubnell, A. J.; Kosnic, E. J.; Squattrito, P. J. *Inorg. Chim. Acta* **1994**, *216*, 101. Kosnic, E. J.; McClymont, E. L.; Hodder, R. A.; Squattrito, P. J. *Inorg. Chim. Acta* **1992**, *201*, 143. Leopard, M. A.; Squattrito, P. J.; Dubey, S. N. *Acta Crystallogr., Sect. C* **1999**, *55*, 35. Gunderman, B. J.; Dubey, S. N.; Squattrito, P. J. *Acta Crystallogr., Sect. C* **1997**, *53*, 17.

- (4) Holman, K. T.; Pivovar, A. M.; Swift, J. A.; Ward, M. D. *Acc. Chem. Res.* **2001**, *34*, 107. Pivovar, A. M.; Holman, K. T.; Ward, M. D. *Chem. Mater.* **2001**, *13*, 3018. Russell, V. A.; Etter, M. C.; Ward, M. D. *J. Am. Chem. Soc.* **1994**, *116*, 1941.
- (5) Côte A. P.; Shimizu, G. K. H. *Coord. Chem. Rev.* **2003**, *86*, 17.
- (6) Cai, J. W.; Chen, C. H.; Liao, C. Z.; Feng, X. L.; Chen, X. M. *Acta Crystallogr., Sect. B* **2001**, *57*, 520.
- (7) Kosnic, E. J.; McClymont, E. L.; Hodder, R. A.; Squattrito, P. J. *Inorg. Chim. Acta* **1992**, *201*, 143. Shubnell, A. J.; Kosnic, E. J.; Squattrito, P. J. *Inorg. Chim. Acta* **1994**, *216*, 101. Gunderman, B. J.; Kabell, Squattrito, P. J.; Dubey, S. N. *Inorg. Chim. Acta* **1997**, *258*, 237. Chen, C. H.; An, D. L.; Gao, S.; Zhu, Z. B.; Huo, L. H.; Zhao, H. *Acta Crystallogr., Sect. E* **2004**, *60*, m11.
- (8) Cai, J. W.; Chen, C. H.; Liao, C. Z.; Yao, J. H.; Hu, X. P.; Chen, X. M. *J. Chem. Soc., Dalton Trans.* **2001**, 1137. Cai, J. W.; Chen, C. H.; Liao, C. Z.; Feng, X. L.; Chen, X. M. *J. Chem. Soc., Dalton Trans.* **2001**, 2370. Chen, C. H.; Cai, J. W.; Feng, X. L.; Chen, X. M. *J. Chem. Crystallogr.* **2001**, *31*, 271.

Table 1. Crystal and Refinement Data

compound	1	2	3	4	5
chemical formula	Ni(Phen)(1,5-NDS)(H ₂ O) ₆ ·NiC ₂₂ N ₂ S ₂ O ₁₂ H ₂₂	Ni(Phen) ₂ (1,5-NDS)H ₂ O·NiC ₃₄ N ₄ S ₂ O ₉ H ₂₄	Co(Phen) ₂ (1,5-NDS)CoC ₃₄ N ₄ S ₂ O ₉ H ₂₂	Ni(Phen) ₂ (2,6-NDS)(H ₂ O) ₃ ·NiC ₃₄ N ₄ S ₂ O ₉ H ₂₈	Co(Phen) ₂ (2,6-NDS)(H ₂ O) ₃ ·CoC ₃₄ N ₄ S ₂ O ₉ H ₂₈
fw	633.28	723.40	705.61	759.43	759.65
cryst syst	monoclinic	triclinic	monoclinic	monoclinic	triclinic
space group	C2/c	P $\bar{1}$	C2/c	P2(1)	P $\bar{1}$
unit cell dimens	<i>a</i> = 20.5536(10) Å <i>b</i> = 12.4245(6) Å <i>c</i> = 12.5312(6) Å β = 124.6030(10)°	<i>a</i> = 8.5615(5) Å <i>b</i> = 12.6265(7) Å <i>c</i> = 14.5058(8) Å α = 89.8730(10)° β = 79.2950(10)° γ = 74.5680(10)°	<i>a</i> = 21.190(6) Å <i>b</i> = 12.590(3) Å <i>c</i> = 14.722(4) Å β = 130.997(3)°	<i>a</i> = 7.8608(5) Å <i>b</i> = 15.3156(10) Å <i>c</i> = 13.5595(9) Å β = 103.2940(10)°	<i>a</i> = 7.7313(6) Å <i>b</i> = 8.3715(7) Å <i>c</i> = 13.348(1) Å α = 106.218(1)° β = 96.410(1)° γ = 101.424(1)°
V (Å ³); Z	2634.0(2); 4	1483.1(3); 2	2964.3(14); 4	1588.72(18); 2	800.21(11); 1
D _x (Mg m ⁻³)	1.597	1.620	1.581	1.588	1.576
abs coeff (mm ⁻¹)	0.962	0.856	0.776	0.807	0.731
F(000)	1312	744	1444	784	391
cryst size (mm ³)	0.10 × 0.10 × 0.05	0.40 × 0.30 × 0.30	0.25 × 0.20 × 0.18	0.10 × 0.04 × 0.04	0.12 × 0.10 × 0.07
θ range (deg)	2.03–28.79	1.68–29.04	3.72–31.05	1.54–29.21	1.61–29.11
limiting indices	−26 ≤ <i>h</i> ≤ 27 −16 ≤ <i>k</i> ≤ 16 −16 ≤ <i>l</i> ≤ 16	−11 ≤ <i>h</i> ≤ 11 −17 ≤ <i>k</i> ≤ 16 −18 ≤ <i>l</i> ≤ 18	−29 ≤ <i>h</i> ≤ 29 −15 ≤ <i>k</i> ≤ 17 −13 ≤ <i>l</i> ≤ 21	−10 ≤ <i>h</i> ≤ 10 −20 ≤ <i>k</i> ≤ 21 −18 ≤ <i>l</i> ≤ 18	−10 ≤ <i>h</i> ≤ 10 −11 ≤ <i>k</i> ≤ 11 −18 ≤ <i>l</i> ≤ 17
radiation type	Mo K α	Mo K α	Mo K α	Mo K α	Mo K α
indep reflns	3224 (<i>R</i> _{int} = 0.1212)	6915 (<i>R</i> _{int} = 0.0404)	4095 (<i>R</i> _{int} = 0.1137)	7429 (<i>R</i> _{int} = 0.0728)	6289 (<i>R</i> _{int} = 0.0491)
refinement method	full-matrix least squares on <i>F</i> ²	full-matrix least squares on <i>F</i> ²	full-matrix least squares on <i>F</i> ²	full-matrix least squares on <i>F</i> ²	full-matrix least squares on <i>F</i> ²
data/restraints/param	3224/0/177	6915/0/434	4095/0/216	7429/1/459	6289/3/451
GOF on <i>F</i> ²	1.065	1.063	1.091	1.088	1.035
Flack param				0.01(2)	0.01(1)
final <i>R</i> indices [<i>I</i> > 2 σ (<i>I</i>)]	<i>R</i> ₁ = 0.047 <i>wR</i> ₂ = 0.11	<i>R</i> ₁ = 0.065 <i>wR</i> ₂ = 0.09	<i>R</i> ₁ = 0.093 <i>wR</i> ₂ = 0.18	<i>R</i> ₁ = 0.094 <i>wR</i> ₂ = 0.12	<i>R</i> ₁ = 0.074 <i>wR</i> ₂ = 0.14
final <i>R</i> indices (all data)	<i>R</i> ₁ = 0.0604 <i>wR</i> ₂ = 0.1215	<i>R</i> ₁ = 0.1131 <i>wR</i> ₂ = 0.1094	<i>R</i> ₁ = 0.1590 <i>wR</i> ₂ = 0.2126	<i>R</i> ₁ = 0.1417 <i>wR</i> ₂ = 0.1331	<i>R</i> ₁ = 0.1081 <i>wR</i> ₂ = 0.1481
largest diff peak and hole (e [−] Å ^{−3})	+0.44 and −0.47	+0.25 and −0.304	+0.96 and −0.38	+0.87 and −0.40	+0.32 and −0.31

up to now do not present direct coordination between the metal and the sulfonate group. Taken together, herein we report the synthesis, crystal structures, and characterization of five novel nickel and cobalt naphthalenedisulfonate compounds, [Ni(Phen)(H₂O)₄](1,5-NDS)·2H₂O (**1**), [Ni(Phen)₂(H₂O)(1,5-NDS)] (**2**), [Co(Phen)₂(1,5-NDS)] (**3**), [Ni(Phen)₂(H₂O)(2,6-NDS)]·2H₂O (**4**), and [Co(Phen)₂(H₂O)(1,5-NDS)]·2H₂O (**5**), as well as their supramolecular extended structures built up by cooperative coordination and other weak intermolecular interactions. The activities of compounds **2–5** as heterogeneous catalysts in the oxidation of organic sulfides have also been tested.

Experimental Section

General Information. All commercially available (Aldrich) products were used without further purification: Ni(NO₃)₂·6H₂O, 99%; Co(NO₃)₂·6H₂O, 98%; 1,5-naphthalenedisulfonate sodium salt (1,5-NDS), 97%; 2,6-naphthalenedisulfonate sodium salt (2,6-NDS), 97%; 1,10-phenanthroline (Phen), 98%. The C, H, and N elemental analyses were performed on a Perkin-Elmer elemental analyzer 2400CHN. IR spectra were recorded from KBr pellets in the range 4000–400 cm^{−1} on a Perkin-Elmer spectrometer. Thermogravimetric and differential thermal analyses (TGA–DTA) were performed using a Seiko TG/DTA 320 apparatus in the temperature range between 25 and 700 °C under a N₂ (flow rate of 50 mL/min) atmosphere and at a heating rate of 5 °C/min.

Synthesis. (a) [Ni(Phen)(H₂O)₄](1,5-NDS)·2H₂O (**1**). Compound **1** was synthesized hydrothermally from an aqueous mixture (6.0 mL) containing Ni(NO₃)₂·6H₂O (0.291 g, 1 mmol), 1,5-

naphthalenedisulfonate sodium salt (0.332 g, 1 mmol), and 1,10-phenanthroline (0.18 g, 1 mmol) in a 30-mL Teflon-lined stainless steel vessel. This vessel was placed in a stainless steel autoclave, sealed, heated to 170 °C under autogenous pressure for 72 h, and cooled to ambient temperature in open air. Green and violet crystals were isolated by decanting the supernatant liquid, washed thoroughly with deionized water, and air-dried. Large green crystals of compound **1** were manually separated from the violet crystals of compound **2**, which always appears in the synthesis, even as majority product.

(b) [Ni(Phen)₂(H₂O)(1,5-NDS)] (**2**) and [Co(Phen)₂(1,5-NDS)] (**3**). The synthesis procedures for compounds **2** and **3** were the same as those used for compound **1** but with a relationship in the initial mixture M²⁺:1,5-NDS:Phen = 1:1:2. Violet crystals of **2** (73% yield) and orange crystals of **3** (56% yield) were obtained after 66 and 72 h, respectively. Elem anal. Calcd for **2**: C, 56.4; N, 7.7; H, 3.3. Found: C, 55.9; N, 7.3; H, 3.2. Calcd for **3**: C, 57.8; N, 7.9; H, 3.2. Found: C, 57.2; N, 6.9; H, 3.3.

(c) [Ni(Phen)₂(2,6-NDS)(H₂O)]·2H₂O (**4**) and [Co(Phen)₂(2,6-NDS)(H₂O)]·2H₂O (**5**). The same synthesis procedure was employed, except now using 2,6-naphthalenedisulfonate sodium salt (M²⁺:2,6-NDS:Phen = 1:1:2) and with heating times of 50 and 24 h, respectively. Violet (86% yield; **4**) and orange crystals (64% yield; **5**) were obtained. It should be emphasized that, with the larger heating time of compound **5**, an impure, more amorphous product is obtained. Elem anal. Calcd for **4**: C, 53.7; N, 7.4; H, 3.72. Found: C, 53.6; N, 7.3; H, 3.7. Calcd for **5**: C, 53.7; N, 7.4; H, 3.7. Found: C, 53.6; N, 7.4; H, 3.7.

Single-Crystal X-ray Diffraction. A summary of the conditions for data collection is given in Table 1. Prismatic crystals of **1–5** were mounted on a Siemens Smart CCD diffractometer equipped with a normal focus, 2.4-kW sealed-tube X-ray source (Mo K α radiation, λ = 0.710 73 Å) operating at 50 kV and 20 mA. Data were collected over a hemisphere of reciprocal space by a

(9) Chen, C. H.; Cai, J. W.; Liao, C. Z.; Feng, X. L.; Chen, X. M.; Ng, S. W. *Inorg. Chem.* **2002**, *41*, 4967. Wang, L.; Yu, X. L.; Cai, J. W.; Huang, J. W. *J. Chem. Crystallogr.* **2005**, *35*, 481.

(10) Cai, J. *Coord. Chem. Rev.* **2004**, *248*, 1061.

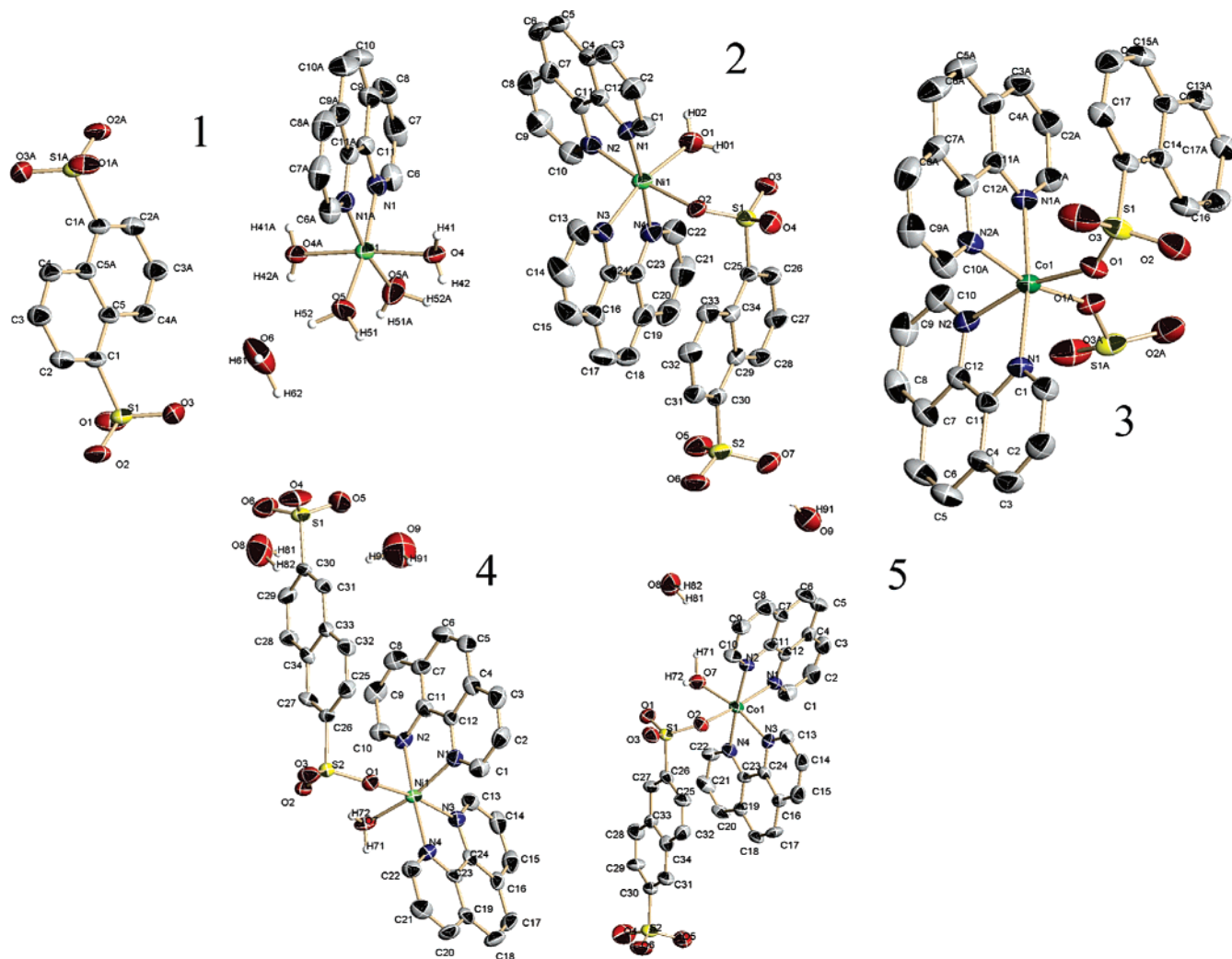


Figure 1. ORTEP drawing and numeration for compounds 1–5.

combination of three sets of exposures. Each set had a different φ angle for the crystal, and each exposure of 20 s covered 0.3° in ω . The crystal-to-detector distance was 5.0 cm. Coverage of the unique set was over 99% complete to at least 23° in θ . Unit cell dimensions were determined by a least-squares fit of 60 reflections with $I > 20\sigma(I)$. The first 100 frames of data were re-collected at the end of the data collection to monitor crystal decay. The intensities were corrected for Lorentz and polarization effects. The structures were solved by Multan and Fourier methods. Full-matrix least-squares refinement with anisotropic thermal parameters for all non-hydrogen atoms was carried out by minimizing $w(F_o^2 - F_c^2)^2$. Hydrogen atoms of the water molecules were located in difference Fourier maps. Calculations were carried out with *SMART* software for data collection and *SHELXTL* for data reduction.¹¹ *ATOMS*¹² was employed for molecular graphics.

X-ray Powder Diffraction. The X-ray powder diffraction patterns were taken at room temperature using a Bruker D8 diffractometer in the step scan mode, with Cu K α ($\lambda = 1.540598$ Å) radiation, and with a step value of 0.02° , measuring for 3 s at each step. The X-ray powder diffraction results were also used to check the purity of the microcrystalline powder by comparison of

the experimental measurements with the simulated X-ray powder diffraction patterns obtained from single-crystal X-ray diffraction.

Catalytic Oxidation Reactions. The flask was charged with (i) a suspension of the catalyst (0.01 mmol) in acetonitrile (3 mL) and (ii) a solution of the substrate (1 mmol) in acetonitrile. The mixture was heated at the desired temperature. Subsequently, the oxidant [H_2O_2 (30%, 3 mmol)] was added, and the reaction mixture was stirred. Chemical yield was measured by gas chromatography.

Results and Discussion

Crystal Structures. Details of cell data, data collection, and refinement are summarized in Table 1. ORTEP drawings of compounds 1–5 with the atomic numbering schemes are shown in Figure 1, and Table 2 shows the coordination distances and angles.

Compound 1 crystallizes in the monoclinic system, space group $C2/c$. Ni^{II} is coordinated to two N atoms of one *o*-phenanthroline molecule and to four O atoms of four water molecules. The 1,5-NDS anion is not directly coordinated to the metallic cation, but it acts as a counteranion. Extensive hydrogen bonds are formed between the complex cations and sulfonate anions through the coordinated water molecules. The result is the creation of a polymeric hydrogen-bonded supramolecular sheet formed by self-assembly of

(11) *Software for the SMART System V5.04 and SHELXTL V 5.1*; Bruker-Siemens Inc.: Madison, WI.

(12) Dowty, E. *ATOMS for Windows 3.1, a computer program for displaying atomic structure*; Kingsport, TN, 1995.

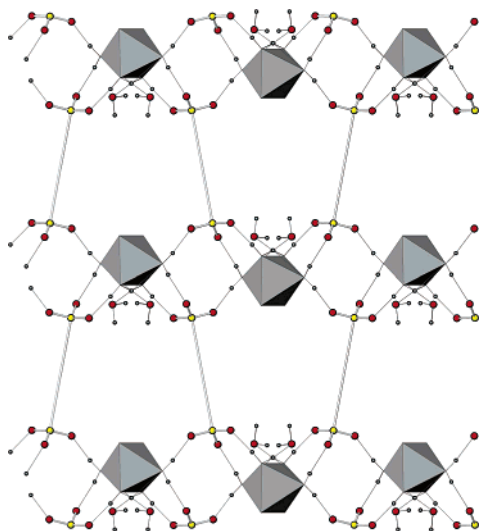


Figure 2. Hydrogen-bonded layer in compound **1**. *o*-Phenanthroline molecules are omitted for clarity, and 1,5-NDS is represented by the S–S axis.

Table 2. Coordination Bond Lengths (Å) and Angles (deg)

Compound 1					
Ni1–N1 × 2	2.074(2)	O5–Ni1–O5'	96.5(1)	N1–Ni1–N1'	80.0(1)
Ni1–O5 × 2	2.057(2)	O5–Ni1–N1 × 2	170.40(9)	N1–Ni1–O4 × 2	95.89(7)
Ni1–O4 × 2	2.087(1)	O5–Ni1–N1' × 2	92.0(1)	N1–Ni1–O4' × 2	88.17(7)
		O5–Ni1–O4 × 2	89.02(8)	O4–Ni1–O4	174.71(9)
		O5–Ni1–O4' × 2	87.46(8)		
Compound 2					
Ni1–N1	2.059(3)	N1–Ni1–N2	80.2(1)	N2–Ni1–O2	171.42(9)
Ni1–N2	2.093(3)	N1–Ni1–N3	96.1(1)	N4–Ni1–N3	80.5(1)
Ni1–N3	2.075(3)	N1–Ni1–N4	175.4(1)	N3–Ni1–O1	166.9(1)
Ni1–N4	2.049(3)	N1–Ni1–O1	94.4(1)	N3–Ni1–O2	83.42(9)
Ni1 O1	2.061(2)	N1–Ni1–O2	91.87(9)	N4–Ni1–O1	89.3(1)
Ni1 O2	2.153(2)	N2–Ni1–N3	100.6(1)	N4–Ni1–O2	91.0(1)
		N2–Ni1–N4	97.2(1)	O1–Ni1–O2	88.55(9)
		N2–Ni1–O1	88.8(1)		
Compound 3					
Co1–N1 × 2	2.136(4)	N1–Co1–O1 × 2	97.0(1)	N2–Co1–O1 × 2	88.0(1)
Co1–N2 × 2	2.138(4)	N1–Co1–O1' × 2	88.7(1)	N2–Co1–O1' × 2	166.1(13)
Co1–O1 × 2	2.106(3)	N1–Co1–N2 × 2	78.0(1)	N2–Co1–N2	97.5(2)
		N1–Co1–N2' × 2	96.7(1)	O1–Co1–O1'	89.6(1)
		N1–Co1–N1'	172.0(2)		
Compound 4					
Ni1–N1	2.093(6)	N1–Ni1–N2	79.7(2)	N2–Ni1–O7	90.5(2)
Ni1–N2	2.060(4)	N1–Ni1–N3	96.7(2)	N3–Ni1–N4	79.7(2)
Ni1–N3	2.073(5)	N1–Ni1–N4	99.4(2)	N3–Ni1–O1	170.4(2)
Ni1–N4	2.056(5)	N1–Ni1–O1	85.7(2)	N3–Ni1–O7	90.1(2)
Ni1–O1	2.110(4)	N1–Ni1–O7	168.6(2)	N4–Ni1–O1	90.8(2)
Ni1–O7	2.107(5)	N2–Ni1–N3	96.3(2)	N4–Ni1–O7	90.8(2)
		N2–Ni1–N4	175.8(3)	O1–Ni1–O7	89.1(2)
		N2–Ni1–O1	93.3(2)		
Compound 5					
Co1–N1	2.148(6)	N1–Co1–N2	78.2(2)	N2–Co1–O7	91.4(2)
Co1–N2	2.091(6)	N1–Co1–N3	96.4(2)	N3–Co1–N4	78.3(3)
Co1–N3	2.126(6)	N1–Co1–N4	99.9(2)	N3–Co1–O2	82.5(2)
Co1–N4	2.118(7)	N1–Co1–O2	168.6(2)	N3–Co1–O7	167.0(2)
Co1–O2	2.160(5)	N1–Co1–O7	94.2(2)	N4–Co1–O2	91.0(2)
Co1–O7	2.098(5)	N2–Co1–N3	98.2(2)	N4–Co1–O7	92.4(2)
		N2–Co1–N4	175.9(3)	O2–Co1–O7	88.6(2)
		N2–Co1–O2	90.7(2)		

tetraaquo-*o*-phenanthroline nickel(II) cations and 1,5-NDS anions (Figure 2). These layers are parallel to the (101) plane. There are also uncoordinated water molecules, which are hydrogen-bonded only with the coordinated ones of the same layer, avoiding, thus, interlamellar hydrogen interactions (Figure 3).

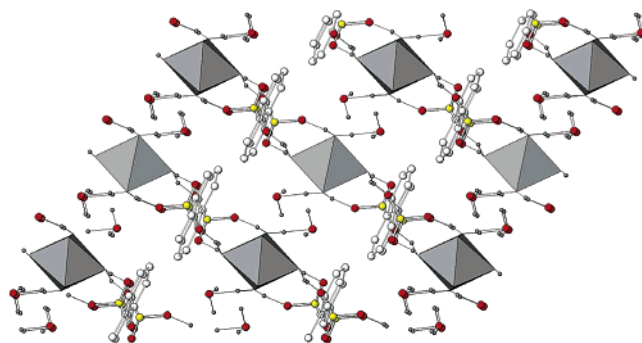


Figure 3. View of the layers in **1** along the [010] direction. *o*-Phenanthroline molecules are omitted for clarity.

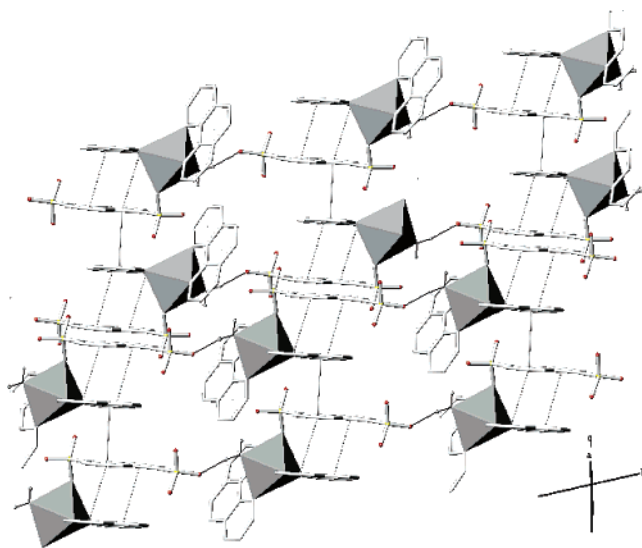


Figure 4. π -Stacking and hydrogen-bond-containing sheets in compound **2**.

Compound **2** crystallizes in the triclinic system, space group $P\bar{1}$. The Ni^{II} ion is in octahedral coordination, bonded to four N atoms of two different *o*-phenanthroline molecules, to one O atom of one 1,5-NDS-sulfonate anion, and to one water molecule. In this compound, the 1,5-NDS-sulfonate linker acts as a monotopic ligand, leaving thus five uncoordinated O atoms. In the structure of compound **2**, the aromatic plane of one *o*-phenanthroline molecule (that containing N3 and N4) and that of the 1,5-NDS ligand are almost parallel (dihedral angle 3.67°). Distances between different ring centroids of these two molecules indicate inter- and intramolecular π - π stacking interactions. The centroids of two rings of the *o*-phenanthroline molecule (C16–C24 and N4–C23 in Figure 1) and those of the 1,5-NDS are at the very short distances¹³ of 3.46 and 3.44 Å, giving rise to a double π intramolecular stacking interaction. The third ring (N1–C24) interacts at 3.53 Å, with one ring of the 1,5-NDS ligand belonging to the nearest-neighbor complex molecule (Figure 4). Besides this intermolecular interaction, as happened in compound **1**, there are hydrogen bonds among the oxygen atom (O1) of the coordinated water molecule and some (O3 and O6) of the uncoordinated sulfonate group, giving rise to 1D chains (Figure 6 and Table 3). As a consequence of the short packing distances, this molecular

(13) Janiak, C. *Dalton Trans.* **2000**, 3885.

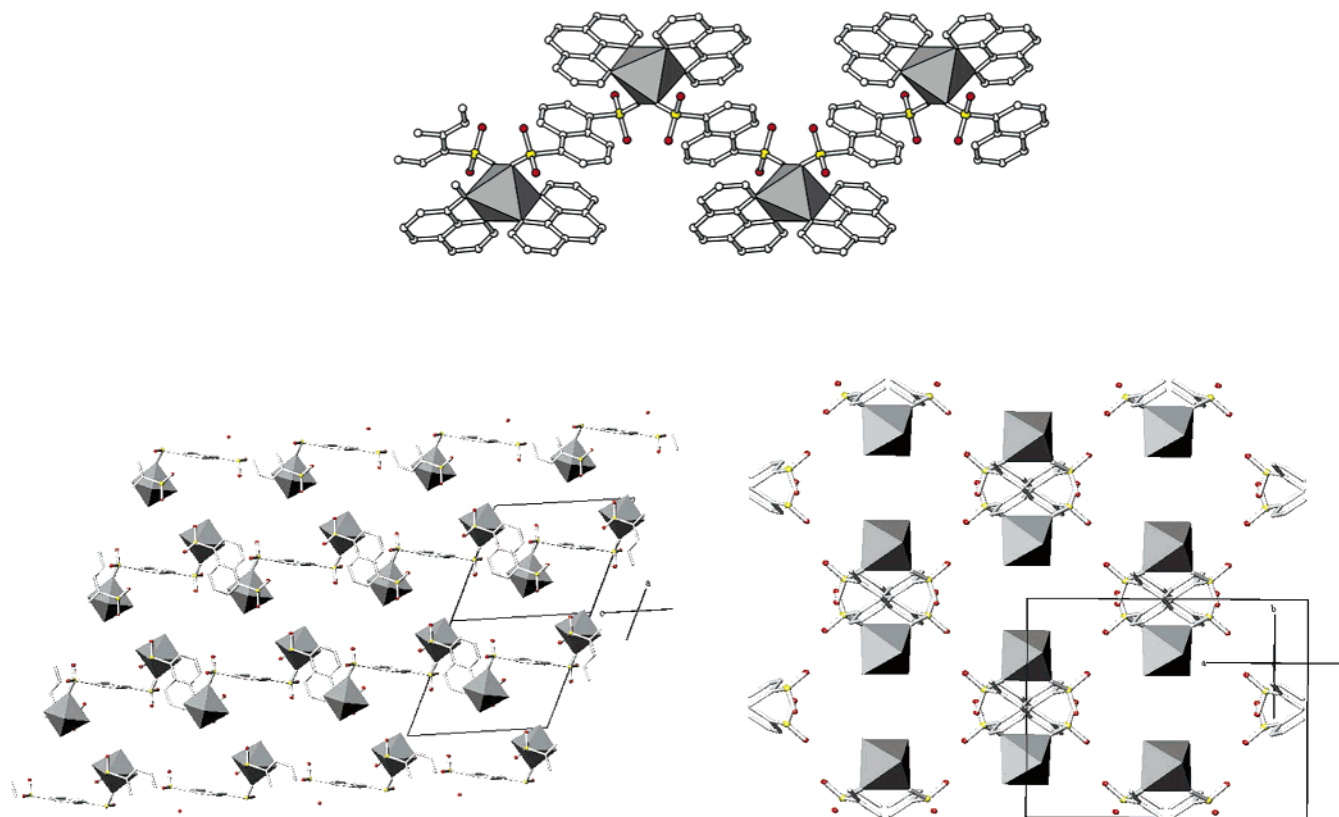


Figure 5. Chains formed in compound **3**, viewed along the $[1,0,-1]$ (top), $[110]$ (bottom left), and $[001]$ (bottom right) directions. *o*-Phenanthroline molecules are omitted in the bottom structures.

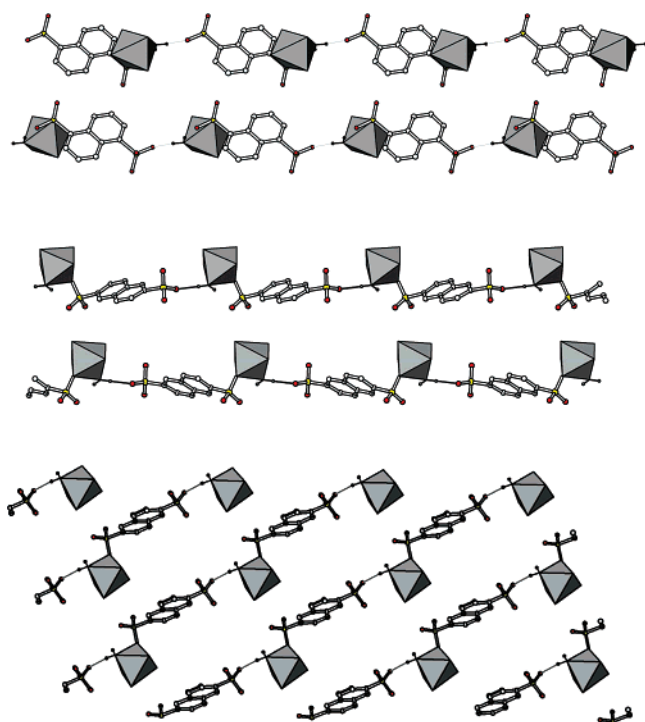


Figure 6. Chains formed in compounds **2**, **4**, and **5** (from top to bottom). *o*-Phenanthroline molecules are omitted for clarity.

complex exhibits a 2D supramolecular structure via $O-H\cdots O$ hydrogen bonds and $\pi-\pi$ perfect face-to-face stacking interactions along the b and a directions, respectively (Figure 4). The role of the second molecule of *o*-phenanthroline as

Table 3. Hydrogen-Bond Interactions for Compounds **1**, **2**, **4**, and **5**

D-H \cdots A	D-H	H \cdots A	D \cdots A	\angle DHA
Compound 1				
O4-H41 \cdots O1 ^I	0.93	1.89	2.724	160
O4-H42 \cdots O2 ^{II}	0.74	2.07	2.804	170
O5-H51 \cdots O3 ^{II}	0.89	1.86	2.694	164
O5-H52 \cdots O6 ^{III}	0.96	1.73	2.694	172
Compound 2				
O1-H01 \cdots O3	0.82	1.96	2.737	158
O1-H02 \cdots O6 ^I	0.83	1.81	2.630	169
Compound 4				
O7-H71 \cdots O4 ^(I)	0.83	1.89	2.726	176
O7-H72 \cdots O2	0.73	2.06	2.765	161
Compound 5				
O7-H71 \cdots O6 ^(I)	1.13	1.62	2.731	168
O7-H72 \cdots O1	0.98	2.01	2.772	133
O8-H81 \cdots O6	1.06	2.49	3.348	137
O8-H82 \cdots O4	1.10	2.01	2.288	134

just a blocking ligand is to avoid any kind of connection along the third direction.

Compound **3** crystallizes in the monoclinic system, space group $C2/c$. As in the Ni compounds, the Co^{II} cation is in octahedral coordination, bonded to the two *o*-phenanthroline chelating molecules and two O atoms of two different sulfonate groups of the 1,5-NDS anion. Contrary to what happens in copper(2+) aminosulfonates, in the current compound, the CoN_4O_2 octahedron is not equatorially coordinated by the four N atoms from the *o*-phenanthroline molecules. The two O atoms being, thus, in the cis position gives rise to a nearly perpendicular arrangement of the 1,5-NDS groups, which behave as bifunctional η^1 spacers, bringing the CoN_4 complex cations into infinite 1D zigzag

strings (Figure 5). Although it has been suggested¹⁰ that the coordination strength of divalent transition-metal ions toward the sulfonate group increases in the order $\text{Co}^{2+} < \text{Ni}^{2+} < \text{Cu}^{2+}$, under our synthesis conditions, this is from the five compounds presented here, the only one in which chains of a covalently bonded metal–NDS spacer appear, and this is, to our knowledge, the first example of a polymeric cobalt sulfonate.

Compound **4** crystallizes in the monoclinic system, space group $P2(1)$. The complex is similar to compound **2**, with the only geometrical differences imposed by the 2,6 position of the sulfonate group. The dihedral angle between the 2,6-NDS and one *o*-phenanthroline molecule planes is a little larger than that in **2**, 9.82° , and a slight slide of one molecule with respect to the other makes the shorter intermolecular interaction distances (four distances are of $3.35\text{--}3.57 \text{ \AA}$) between their aromatic rings in this compound centroid–C instead of centroid–centroid, in a $\pi\text{--}\pi$ slipped stacking. One intramolecular $\pi\text{--}\pi$ stacking interaction (3.54 \AA) appears in this compound, too. Similarly to compound **2**, chains through hydrogen bonds are formed, but in the current compound, they run along the *c* direction (Figure 6 and Table 3). In summary, the packing of **4** exhibits a 2D supramolecular structure via $\text{O}\text{--}\text{H}\cdots\text{O}$ hydrogen bonds and $\pi\text{--}\pi$ stacking interactions along the *c* and *a* directions, respectively. The second molecule of *o*-phenanthroline avoids connections along the third direction in **4**, too.

Compound **5** crystallizes in the triclinic system, space group $P\bar{1}$. The coordination of the metal atom is the same as that in compounds **2** and **3**. The dihedral angle of the planes formed by 2,6-NDS and one *o*-phenanthroline molecule is 5.55° . In this structure, inter- and intramolecular interactions among aromatic rings indicate a $\pi\text{--}\pi$ parallel-displaced stacking along the *b* direction. Hydrogen bonds between the coordinated water molecule O7 and sulfonate group O atoms form chains along the $[011]$ direction and via one of the noncoordinated water molecules O8 along the *a* direction. None of the *o*-phenanthroline molecules avoids connections in the third direction, allowing, thus, the formation of a 3D supramolecular self-assembly via $\text{O}\text{--}\text{H}\cdots\text{O}$ hydrogen bond layers and $\pi\text{--}\pi$ parallel-displaced stacking interactions (Figure 7). Figure 6 shows the different chains formed in compounds **2**, **4**, and **5**.

X-ray Powder Diffraction. Comparative experimental and simulated (on the basis of the crystal structures) powder patterns show the high level of purity of compounds **2–5**. The powder pattern of compound **1** presents a pick at $2\theta = 12.4^\circ$ corresponding to the most intense peak of compound **2**, which is always present in the synthesis product, as was previously explained in the Experimental Section.

IR spectra of **1–5** are very similar and present both ν_{as} and ν_{s} of the sulfonate groups found at $\sim 1260\text{--}1120$ (ν_{as}) and $\sim 1030 \text{ cm}^{-1}$ (ν_{s}), with the aromatic C–H stretching mode being situated in the area of $3150\text{--}3000 \text{ cm}^{-1}$. The IR spectra of these compounds show additional bands at ca. $3600\text{--}3100 \text{ cm}^{-1}$, which correspond to the water molecules.

TGA–DTA studies of the four compounds (**2–5**) obtained as pure phases have been performed under a N_2 flow

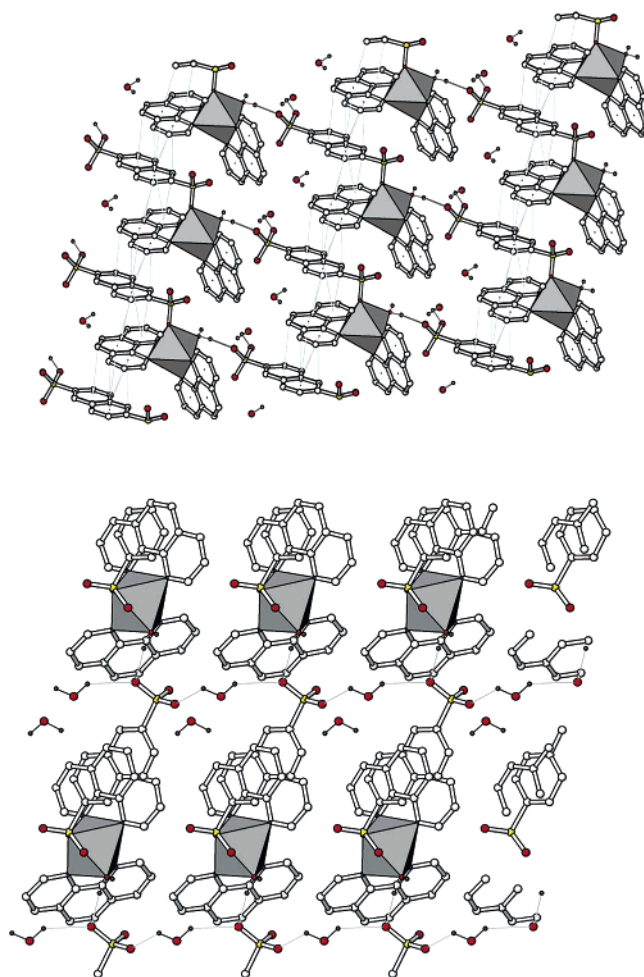


Figure 7. 3D structure of compound **5**: (top) *bc* plane showing π stacking and hydrogen bonds; (bottom) hydrogen-bond connections along the $[100]$ direction.

on the as-synthesized products, which had proven to be quite pure according to the elemental analysis and X-ray powder diffraction measurements. Compound **2** loses its only water molecule at the substantially high temperature of $270 \text{ }^\circ\text{C}$ (found 3%, calcd 2.5%), and then the product remains stable up to $\sim 500 \text{ }^\circ\text{C}$, while in compound **3**, no weight loss is observed below $450 \text{ }^\circ\text{C}$, the temperature at which the product begins to decompose. In compounds **4** and **5**, the weight losses corresponding to totally three water molecules are observed at $\sim 240 \text{ }^\circ\text{C}$ (**4**) and $\sim 200 \text{ }^\circ\text{C}$ (**5**) (found 6.5%, calcd 7.1% for **4**; found 6.9%, calcd 7.1% for **5**). The decomposition temperatures for these compounds are ~ 460 and $\sim 420 \text{ }^\circ\text{C}$, respectively.

Catalytic Reactions. Sulfoxides are known to have interesting and useful biological and pharmacodynamic properties¹⁴ as well as being the most widely used chiral auxiliaries.^{15,16} They are obtained by oxidation of thioethers by peracids, peroxides, and alkyl peroxides using transition-

(14) Renwick, A. G. In *Sulfur-containing Drugs and Related Organic Compounds*; Damani, L. A., Ed.; Ellis Horwood: Chichester, England, 1989; Vol. 1, Part B, p 133.

(15) Mikołajczyk, M.; Drabowicz, J.; Kielbasinski, P. *Chiral Sulfur Reagents. Application in Asymmetric and Stereoselective Synthesis*; CRC Press: Boca Raton, FL, 1997.

(16) Carreño, M. C. *Chem. Rev.* **1995**, *95*, 1717.

Table 4. Results Obtained in the Oxidation of Methyl Phenyl Sulfide with H₂O₂ Promoted by Ni- and Co-NDS Catalysts

catalyst	convn (%) (6 h) ^a	TOF (h ⁻¹) ^b	selectivity (%) ^c
2	97	5	82
3	62	2	96
4	100	22	100
5	100	48	100

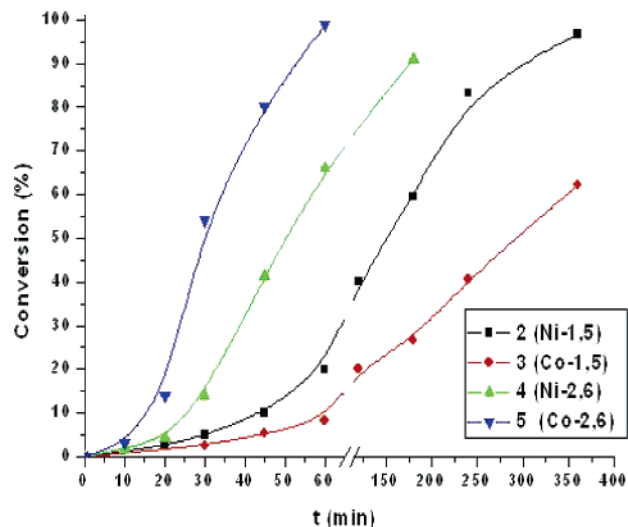
^a Conversion determined by gas chromatography–mass spectrometry.

^b TOF: millimoles of substrate per millimoles of catalyst per hour. ^c Amount of sulfoxide/amount of sulfide consumed.

metal catalysts.¹⁷ Depending on the catalyst selectivity and the method used, different proportions of sulfoxide and sulfone are produced. Among the metal catalysts for asymmetric sulfide oxidation, Ti-based systems are the most prominent ones.^{18,19} Homogeneous catalysis often provides the best results in achieving high levels of selectivity, whereas heterogeneous catalysis offers the advantages of simplified product purification and the potential for catalyst recycling.²⁰ Clearly, heterogeneous catalysis, which can provide high selectivity, would be an important development with potential applications in industrial and high-throughput organic chemistry.²¹

The catalytic activities of compounds 2–5 were examined for the oxidation of organic sulfides (methyl phenyl sulfide), and the results are summarized in Table 4. Hydrogen peroxide (H₂O₂) acts as an oxidant in acetonitrile, yielding high conversion at low temperature. A series of blank experiments revealed that each component is essential for an effective catalytic reaction and the system is relatively unaffected by changing the order of mixing. Catalysts 2–4 appeared to be stable under experimental conditions (the catalysts were recovered by filtration of the reaction mixture, washed with acetonitrile, and checked by X-ray powder diffraction) but were found to be reactive for a further catalytic run. Complex 5 is soluble in the reaction media probably because of oxidative degradation during the oxidation reaction.

The main product of oxidation of alkyl phenyl sulfide is sulfoxide. The product of oxidation of sulfoxide was mainly formed at conversions higher than 80%. No significant changes in the product distribution are observed when the whole amount of oxidant is added in one single stage or gradually added during the course of the reaction. To determine any matrix effects on the rate of the reaction, the kinetics curves of the oxidation of methyl phenyl sulfide catalyzed by Ni and Co catalysts were compared (Figure 8).

**Figure 8.** Kinetic profile for the oxidation of methyl phenyl sulfide with Ni and Co catalysts.

The conversions of sulfide to sulfoxide were found to decrease over the polymeric Co complex 3, whereas when using Co complex 5 as the catalyst, an important increase for the catalytic activity was found. This latter being soluble in the reaction media acts like any other homogeneous catalyst. From a mechanistic point of view, the sulfoxidation reaction must go, as usual,²¹ through the corresponding oxo complex active species, which explains the lower activity and longer induction period of the reaction when using 3. In this compound, the lack of easily displaceable coordinated water molecules makes intermediate species formation difficult. The two Ni complexes 2 and 4 are better heterogeneous catalysts, and among them, that of 2,6-NDS is the most active.

Recycling a Heterogeneous Catalyst. The major advantage of the use of heterogeneous catalysts is the ease with which they can be recovered from the reaction mixtures by simple filtration and reused. The heterogeneous oxidation of sulfides has been carried out until completeness. The catalysts were filtered and washed, and then fresh substrate and solvent were added without further addition of any catalyst, for several consecutive experiments; yield, activity, and selectivity were all retained. After each experiment, a portion of the catalyst was analyzed to determine that the structure was not changed. Filtrates were used in new reactions and were not found to catalyze oxidation.

Conclusions. By introduction of 1,10-phenanthroline into the reaction mixture in a *o*-phenanthroline/sulfonate ratio of 2:1, compounds 2–5 were obtained, while by using a 1:1 ratio, a tetraquo-*o*-phenanthroline-nickel salt (compound 1) was obtained. In structures 2–5, the metal is 6-coordinated by four N atoms of the two *o*-phenanthroline ligands, but in none of them are these molecules occupying the four equatorial positions, as occurs in many other complexes with N-containing auxiliary ligands. Independently, it is the 1,5- or 2,6-NDS anion that coordinates in the four compounds in a η^1 mode. Self-assembly interactions of all of the five compounds were studied: one of them (1) is a polymeric hydrogen-bonded supramolecular layered compound formed

(17) Oae, S. *Organic Sulfur Chemistry: Structure and Mechanism*; CRC Press: Boca Raton, FL, 1991; Chapter 6.

(18) Bonchio, M.; Licini, G.; Modena, G.; Bortolini, O.; Moro, S.; Nugent, W. A. *J. Am. Chem. Soc.* **1999**, *121*, 6258.

(19) Massa, A.; Siniscalchi, F. R.; Bugatti, V.; Lattanzi, A.; Scettri, A. *Tetrahedron: Asymmetry* **2002**, *13*, 1277.

(20) Blaser, H. U.; Pugin, B. In *Chiral reactions in heterogeneous catalysis*; Jannes, G., Dubois, V., Eds.; Plenum Press: New York, 1995; p 33. *Chiral Catalyst Immobilization and Recycling*; Vos, D. E., Vankelecom, I. F. K., Jacobs, P. A., Eds.; Wiley-VCH: Weinheim, Germany, 2000.

(21) Sheldon, R. A.; van Bekkum, H., Eds. *Fine Chemicals through heterogeneous catalysis*; Wiley-VCH: Weinheim, Germany, 2001. Arends, I. W. C. E.; Sheldon, R. A. *Appl. Catal.* **2001**, *212*, 175. Ayala, V.; Corma, A.; Iglesias, M.; Sánchez, F. *J. Mol. Catal. A: Chem.* **2004**, *221*, 201; *Dalton Trans.* **2001**, 2370.

by self-assembly of tetraaquo-*o*-phenanthroline nickel(II) cations and 1,5-NDS anions, two (**4** and **2**) are also 2D structures via O–H···O and π – π stacking interactions, and one (**5**) presents a 3D structure via O–H···O hydrogen-bond layers and π – π parallel-displaced stacking interactions. Compound **3** is the first example of one covalently bonded polymeric cobalt sulfonate. Its 1D structure comprises chains formed through bitopic 1,5-NDS linkers.

The catalytic activities of compounds **2**–**5** were checked for oxidation of organic sulfides. The two Ni complexes **2** and **4** are better heterogeneous catalysts, and among them, that of 2,6-NDS is the most active.

Acknowledgment. F.G. acknowledges a FPI fellowship from Spanish Ministry for Education and Science

(MEC) cofunded by Fondo Social Europeo. This work has been supported by the Spanish MCIT Project Mat 2004-2001.

Supporting Information Available: Comparative simulated–experimental powder patterns of compounds **1**–**5** and X-ray crystallographic data in CIF format. This material is available free of charge via the Internet at <http://pubs.acs.org>. CCDC reference numbers 604189, 604190, 604191, 604192, and 604193 contain the supplementary crystallographic data for this paper. These data can be obtained free of charge from the Cambridge Crystallographic Data Centre, 12 Union Road, Cambridge CB21EZ, U.K., fax (-44)1223-336-033.

IC060897M